PERGAMON

Radiation Measurements 35 (2002) 433–438

Radiation Measurements

www.elsevier.com/locate/radmeas

Dosimetry inside MIR station using a silicon detector telescope (DOSTEL)

R. Beaujean[a,*], J. Kopp[a], S. Burmeister[a], F. Petersen[a], G. Reitz[b]

[a] *Institut für Experimentelle und Angewandte Physik, Universität Kiel, 24109 Kiel, Germany*
[b] *Institut für Luft- und Raumfahrtmedizin/Strahlenbiologie, DLR, 51140 Köln, Germany*

Received 26 January 2001

Abstract

The dosimetry telescope (DOSTEL)was flown on the MIR orbital station during October 1997–January 1998. The mission average contributions to the absorbed dose rates (in water) were 126 ± 4 μGy/d and 121 ± 13 μGy/d for the GCR and the SAA component, respectively. The mean quality factors (ICRP60) deduced from the LET-spectra are 3.5 ± 0.2 (GCR) and 1.3 ± 0.1 (SAA). Separate LET spectra and temporal variations of the absorbed dose rates and of the mean quality factors are presented for these two radiation components as well as for solar energetic particles of the November 6, 1997 event.

Keywords: Space flights; Active dosimetry; Silicon detectors; Dose equivalent; LET-spectra

1. Introduction

As radiation is a primary concern for manned spaceflight and is a potentially limiting factor for long-term orbital and interplanetary missions, dosimeters are part of each manned spaceflight mission. Passive detectors like TLDs, plastic nuclear track detectors and nuclear emulsions accumulate the absorbed dose and require recovery for the data analysis (unless special inflight analysis by the crew is provided). Active dosimetry provides real-time information on temporal changes of the dose rate and can be operated without any crew activity.

The complex radiation environment during space missions in low-Earth orbits (LEO) has large temporal variations in intensity and composition and it is unique and not comparable to the terrestrial radiation. The main contribution to the absorbed dose in LEO comes from energetic charged particles of (a) the galactic cosmic rays (GCR), (b) the Earth's radiation belt and (c) sporadic solar particle events. In addition to these main constituents, albedo neutrons from GCR interaction with the Earth's atmosphere, secondary particles from interactions in the shielding matter, and electromagnetic radiation are present. Additional information on the radiation field and the influence of solar modulation, geomagnetic field effects and material shielding is given elsewhere (Beaujean et al., 1995; Badhwar, 1997).

Besides providing information on temporal changes of the dose rate in orbit, dosimetry with active detectors can monitor the "quality" of the radiation by measuring the Linear Energy Transfer (LET) distribution. This information is necessary to obtain the dose equivalent using LET dependent quality factors (ICRP, 1991).

Radiation measurement with planar silicon detectors is one approach to active space dosimetry. The detector system is stable, easy to handle and it provides information which is necessary for radiation protection. However, planar silicon detectors have the deficiency that they are not tissue-equivalent and that their count rates are attitude sensitive in a radiation field which is not isotropic. The charged-particle telescope DOSTEL was developed in 1995 as a small size, low budget instrument for flights in the ESA Biorack. NASDA has flown a more complex charged-particle telescope based on position-sensitive

* Corresponding author. Tel.: +49-431-880-2544; fax: +49-431-880-2547.
E-mail address: r.beaujean@email.uni-kiel.de (R. Beaujean).

1350-4487/02/$ - see front matter
PII: S1350-4487(02)00074-4

silicon detectors (Doke et al., 2001a) while NASA has used a tissue-equivalent proportional counter (TEPC) for space dosimetry (Badhwar et al., 1996)

2. Instrumentation

The DOSimetry TELescope DOSTEL is based on two identical passivated implanted planar silicon (PIPS) detectors (Canberra Semiconductors) and designed to measure the energy deposition of charged particles. Both detectors have a thickness of 315 μm and a sensitive area of 693 mm^3. The distance of 15 mm between the two detectors yields an geometric factor of 824 mm^2 sr for particles arriving from the front when a coincidence in both detectors is required. In the experiment, Active Dosimetry of Charged Particles (ADCP) which was flown as part of the NASA-6 mission on MIR station in the Kristall module during October 1997 to January 1998, the DOSTEL detectors were alligned with a telescope of three CCD-detectors. This mounting results in a different shielding for particles impinging from the front and the rear. However, the instrument could not determine the arrival direction of the individual particles. In this report, only results of the measurement with the two DOSTEL detectors are presented.

The electronic design for the DOSTEL unit as part of the ADCP experiment was almost identical to the original version which was flown in the Biorack facility of the European space agency (ESA) on space shuttle missions STS-76, -81 and -84 (Beaujean et al., 1999b). Each detector is connected to an independent analogue signal section consisting of a charge sensitive amplifier (CSA) with 2pF integrating capacitor followed by a two-step pulse amplifier (PA1, PA2) and two peak detectors. For noise reduction purposes, two RC-filters with equal individual time constants of 1 μs are included in each detector signal line. Together with a multiplexed 8-bit ADC this design allows a pulse height analysis of the detector signals with different resolution for the low and high energy deposition region.

The DOSTEL version on MIR station had different gain factors (PAl × PA2) of 4 × 30 (Dl, top) and 10 × 20 (D2, bottom) for the individual detectors. Compared to earlier versions of DOSTEL, this new design extends the Linear Energy Transfer (LET) range (in water) covered by the instrument to 0.1–240 keV/μm for Dl and narrows it to 0.07–95 KeV/μm for D2 where the resolution became higher. For dose measurements all LET values exceeding the upper limit LET_{max} are taken as LET_{max}.

The digital signal section was unchanged using the main components 8-bit MCU (68HC711), timer (68HC68T1), 1 MB flash memory (E28F008SA) and 32 kB RAM (CXK58257AM-10LL). Scientific and housekeeping data for a 10-day period can be stored in the flash memory, after this period data had to be downloaded via the RS232 interface to an independent storage. No malfunction of the electronics due to single event upsets (SEU) were detected

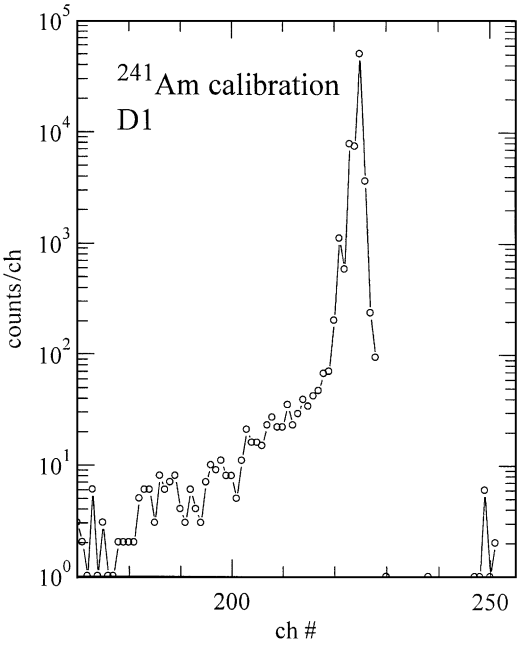

Fig. 1. Pulse height distribution of stopping alpha particles from ^{241}Am in detector D1 (pressure 0.1 mbar, distance 10 cm).

during the 87-days mission on MIR station (as before on the three 10-days shuttle missions). The total power consumption of DOSTEL is 0.7 W from ±10 V DC and +5 V DC.

Before the final assembly on top of the CCD telescope, the energy deposition response of the signals from the two DOSTEL detectors was calibrated by exposure to ^{241} Am in a vacuum chamber (pressure 0.1 hPa, distance 10 cm). Fig. 1 shows the result for detector Dl. Because the dead layer of the detectors is specified at about 0.1 μm, it can be neglected and the peak is attributed to stopping alpha-particles of 5.48 MeV (their range in Si is about 28 μm). Also the two other energies at 5.44 MeV (13%) and 5.39 MeV (1.3%) can be identified, however, the resolution is not sufficient to resolve these lines. For these calibration measurements with ^{241}Am the gain of the pulse amplifiers was reduced in order to yield the 5.48 MeV peak at the high end of the low-energy deposit channels. Thus, this method calibrates the CSA sensitivity including the RC-filter attenuation and the peak detectors. The ultimate response is calculated from the nominal gain of the pulse amplifiers which is better than 2%. The overall linearity for the low and high energy deposit range was verified by using test pulses from a tail pulse generator.

3. Measurements

On orbit, particle and absorbed dose rates are registered for time intervals of 100 s in the two detectors separately without coincidence requirement while energy deposition

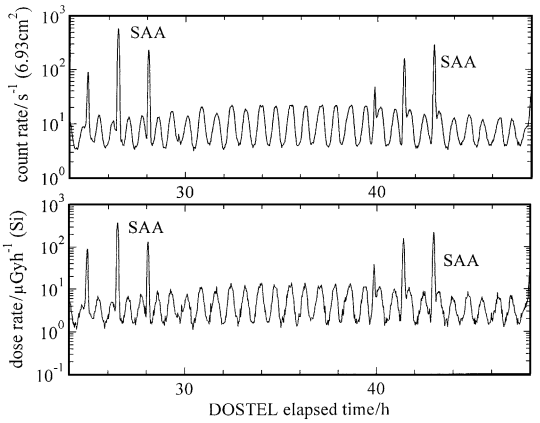

Fig. 2. Typical temporal variation of count rate (top) and dose rate (bottom) during 24 h quiet time inside Kristall module on MIR.

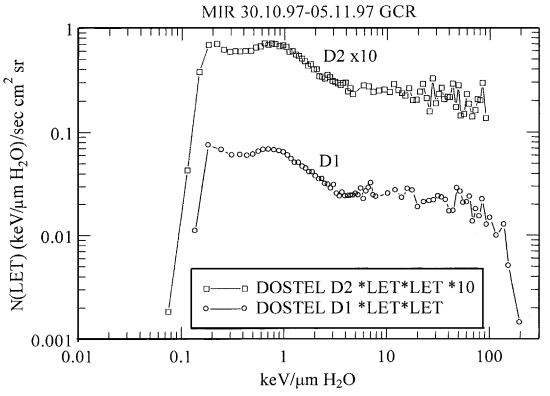

Fig. 3. Comparison of LET-measurements for GCR particles in the coincidence mode. The individual detectors D1 and D2 cover different LET ranges in the low and height LET region.

distributions from coincident events in both DOSTEL detectors were integrated over periods of half-orbits in the northern and the southern magnetic hemispheres separately. These time intervals for the energy deposit distributions are defined by the count rate minima at crossings of the magnetic equator. A special data sampling mode for crossing of the radiation belt in the region of the South Atlantic Anomaly (SAA) is entered when the particle rate exceeds a threshold value of 50 counts/s. Then the particle and dose rates are measured in 20 s time intervals and a separate energy deposit spectrum is integrated until the count rate drops below 25 counts/s. The same mode was entered when high particle fluxes were encountered at high latitudes during the solar particle event of November 6, 1997.

Fig. 2 is an example of the count rate and dose rate (measured in Si) versus elapsed time during quiet solar period. It shows the temporal variations due to changing magnetic cutoff conditions (minima at the magnetic equator every 45 min and maxima at high latitude positions) and pronounced peaks during crossing of the SAA region about 6–8 times per 24 hours. The two groups of SAA peaks clearly show the ascending and descending orbit sections with declining and increasing GCR rates, respectively. As the period for one orbit (51.6 deg inclination at an altitude of about 380 km) is close to 90 min, one day contains 16 orbits and the daily pattern is similar due to the similar ground tracks after 16 revolutions. Dose rates in the individual detectors are measured in the single-detector mode, i.e. no coincidence between detectors Dl and D2 is required. This allows measurement of nearly correct dose rates in the radiation belts where the radiation field is not isotropic.

Fig. 3 shows typical differential distributions $N(LET) * LET * LET$ in Dl and D2 for particles measured in the northern hemisphere (GCR). LET(Si) values are deduced from the measured energy deposited in the individual silicon detectors in coincidence mode using a mean pathlength of 364 μm at a density of 2.33 g/cm^3. This procedure underestimates the LET value of short range particles stopping inside the detector. In order to account for the difference in stopping power of Si and water, the LET(Si)-value is multiplied by a factor of 1.23 to get the LET(H_2O)-value. This conversion factor is applied throughout this report as a mean value for all calculations of LET(H_2O)-spectra neglecting that the factor depends on the particle's energy and therefore depends on shielding especially for the SAA-contribution (Atwell, 2001). The uncertainty of this revised conversion factor is estimated to be 3% (a factor of 1.31 was used in our earlier data analysis).

The figure displays the different low and high LET ranges covered by the individual detectors due to the difference of the pulse amplifier gain factors and verifies that almost identical spectra are measured in Dl and D2 over the common LET range. The sensitivity of detector D2 in the low-LET region is sufficient to resolve the peak of minimum ionizing particles ($Z = 1, v/c \cong 1$) while Dl covers the high-LET range up to LET(H_2O) = 240 keV/μm.

A major solar particle event occurred on November 6, l997 providing a rare occasion to sample dosimetric data of this unpredictable constituent of the radiation environment in space. During the onset of this event, the MIR station was in an orbit which reached the polar caps at high magnetic latitude segments where the geomagnetic shielding of charged particles has its lowest values. Therefore, the onset of this event could be observed by our instrument inside the station as shown in Fig. 5. Our data from the latter portion of the event were lost due to external storage problems.

4. Results and discussion

Fig. 4 shows differential linear energy transfer (LET) spectra in detector D2 for the GCR, SAA and SEP contributions measured in the coincidence mode. D2 has the best resolution in the low LET region. The SEP spectrum is

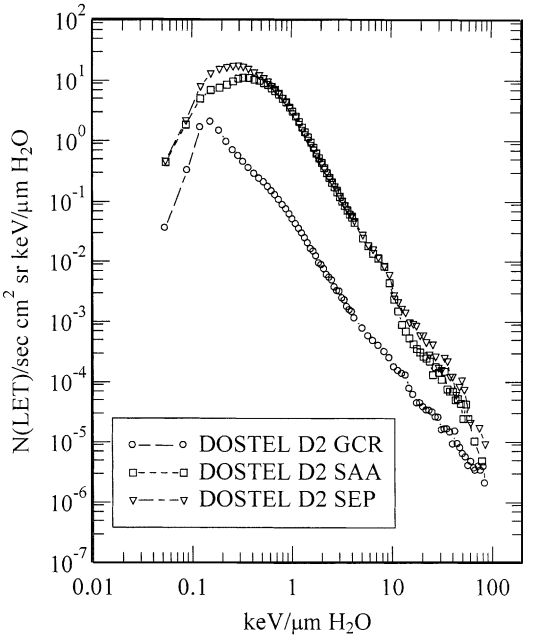

Fig. 4. LET spectra from detector D2 for three radiation components (GCR, SAA, SEP). See text for the discussion of the relative abundances.

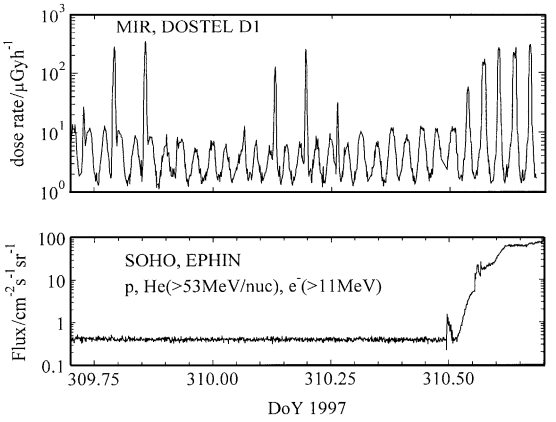

Fig. 5. Temporal variation of absorbed does rates for the November 6 solar particle event inside MIR (top) and interplanetary particle fluxes on SOHO (bottom, Mueller-Mellin, 2001).

derived from measurements in the five consecutive peaks during the onset of the November 6 event (Figs. 5 and 6) when the instrument changed to the SAA mode. The latitudes for these segments are estimated to be greater than 45 degree (geographic). The GCR spectrum is calculated with a geometric factor of 824 mm^2 sr which neglects albedo particles and deviation from a 2π-geometry in low-Earth orbits during horizontal viewing directions of the telescope. While the time intervals for the GCR measurement are well defined, the time intervals for the SAA and SEP measure-

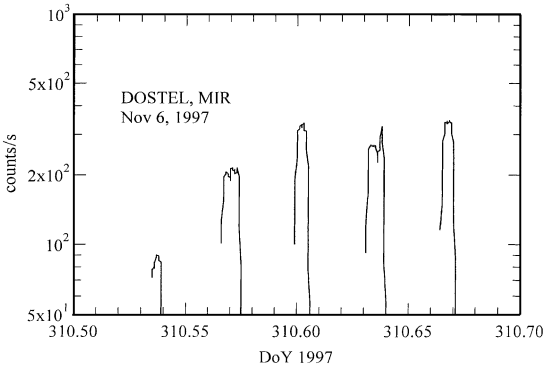

Fig. 6. Detailed structure of the DOSTEL peak count rates during the onset of the November 6 solar particle event.

ments depend on the selected count rate threshold for a mode change. This selection procedure excludes low fluxes and yields overestimated mean differential fluxes. Another concern is the value of the solid angle for the SAA distribution. Since the coincidence mode restricts the arrival direction of the accepted particles, the event rates in this mode strongly depend on the viewing direction. This effect was verified inside the ESA Biorack by simultaneous measurements with two DOSTEL units at different viewing directions during crossings of the SAA (Beaujean et al., 1999a).

Therefore, only the shape of the spectra should be considered for comparison but not the absolute numbers. The shape of the curve defines the mean quality factor Q and it is obvious that the GCR spectrum has the lowest gradient and thus the highest Q value. For a given LET spectrum the calculated Q value depends on the LET range of the measurements. DOSTEL covers a range of 0.1–240 keV/µm (water) in detector Dl and the Q values in Table 1 are based on this LET range neglecting the overflow counts. The GCR spectrum shows a peak value slightly below the calculated LET = 0.2 keV/µm value for relativistic singly charged particles. This is attributed to the Landau-distribution of energy losses and the applied mean path length of 364 µm.

Assuming a power law the LET spectrum can be extrapolated and the overflow counts can be used to extend the measured spectrum. For example, this procedure leads to an increase of the mean quality factor from 3.32 to 3.52 for the GCR measurement for the period November 30–December 4 (ICRP60).

Table 1 summarizes absorbed dose rate values measured in silicon and calculated dose equivalent rates in water for detector Dl in the LET-range 0.1–0.24 KeV/µm. The GCR average dose rates were measured during half orbits in the northern magnetic hemisphere and subtracted from the measured mission average dose rate in order to deduce the value called SAA average dose rate. For the GCR and SAA contribution the measured LET spectra (Fig. 4) are used to calculate the mean quality factors Q (ICRP60, 1991) and the dose equivalent rates. The statistical uncertainty of the Q

Table 1
Dose rates (in Si), dose equivalent rates and mean quality factors Q (ICRP60) in detector D1 for different periods during the mission

Period	Mission average			GCR average			SAA average		
	μGy/d (Si)	Q	μSv/d	μGy/d (Si)	Q	μSv/d	μGy/d (Si)	Q	μSv/d
10.10–14.10.1997	201	2.5	617	97	3.7	444	104	1.4	173
15.10–19.10.1997	203	2.4	589	105	3.3	433	97	1.3	156
20.10–22.10.1997	186	2.6	599	104	3.6	463	83	1.3	137
25.10–29.10.1997	207	2.4	604	105	3.5	449	101	1.2	154
30.10–01.11.1997	226	2.1	590	105	3.2	407	121	1.2	184
05.11–06.11.1997	260	2.4	764	102	3.9	495	157	1.4	269
14.11–19.11.1997	200	2.5	615	105	3.6	469	96	1.3	147
22.11–29.11.1997	208	2.2	557	100	3.2	396	107	1.2	161
30.11–04.12.1997	212	2.2	578	101	3.3	412	111	1.2	166
05.12–09.12.1997	191	2.6	617	97	3.7	440	94	1.5	176
10.12–14.12.1997	202	2.4	605	102	3.5	443	101	1.3	162
15.12–19.12.1997	209	2.4	619	99	3.7	453	110	1.2	166
20.12–24.12.1997	184	2.5	570	100	3.5	425	85	1.4	145
25.12–29.12.1997	198	2.5	613	105	3.6	465	93	1.3	148
30.12–03.01.1998	206	2.5	644	107	3.8	497	99	1.2	148
06.01–14.01.1998	192	2.6	602	105	3.5	456	87	1.4	146
15.01–19.01.1998	194	2.6	614	102	3.8	473	92	1.3	141

values is about 0.2 and 0.03 for GCR and SAA respectively. For the mission average numbers, the quality factor is the ratio of the given dose equivalent rate (sum of the GCR and SAA dose equivalent rates) and the measured dose rate (converted to water by applying the factor 1.23). This procedure assumes equal GCR contributions on either magnetic hemispheres and is independent of the selected threshold for the mode change. However, it is not applicable during the SEP event and therefore data of the concerned period should be neglected here.

The GCR dose rate remained almost constant at a mean value of 126 μG/d (water) with a standard deviation of 4 μG/d. The mean value for the SAA contribution after November 10 is 121 μG/d with a standard deviation of 13 μG/d. The errors are purely statistical and do not include any calibration error. As the SAA contribution comes from the inner radiation belt, the SAA measurement is biased by two effects. For each SAA crossing the integrated dose value depends on (a) the individual ground track and (b) to a certain extent on the viewing direction of the telescope relative to the magnetic field line. The trapped protons are confined close to the mirror plane—perpendicular to the magnetic field vector—at this low altitude. Therefore, the particle arrival direction is not isotropic and the count rate strongly depends on the orientation of the planar detector. Different amounts of shielding at different particle arrival directions and temporal variations of the atmospheric density (Badhwar, 1997) must also be considered. Although the dose rate in the single detector mode is almost independent of the orientation of the planar detector, the measurements during periods of 5 days show a considerable variation due to the discussed effects.

Up to now, we do not know details about the amount of shielding at the DOSTEL position in the Kristall module and on the position and attitude of the MIR station. Therefore it is difficult to discuss the results on dose rate measurements in comparison to other instruments on different missions (Doke et al., 2001a, Badhwar et al., 1996). Compared to DOSTEL data from Shuttle-to-MIR missions (Beaujean et al., 1999a), the MIR measurement for GCR is in agreement to our previous results. Taking into account the almost constant modulation level during the solar minimum period of 1996/1997, this indicates only minor changes of the average shielding conditions in the different missions. However, the SAA contribution on MIR is significantly smaller than previously measured with the same instrument aboard the NASA-Shuttle on similar orbits. This may be explained by differences in altitude and attitude (which could not be verified for lack of position data) and potential differences in the shielding distribution.

Fig. 5 shows the available DOSTEL dose rate data of the November 6 solar particle event. The maximum peak dose rate of almost 300 μGy/h is in reasonable agreement with the NASA TEPC measurement (Badhwar, 1998). Analysis of the LET spectrum at 0.1–240 KeV/μm (Fig. 4) yields a mean quality factor of 1.55 ± 0.07 (ICRP60) while Badhwar (1998) reported $Q = 1.93$ for LET = 0.3–220 keV/μm. This higher quality factor of the TEPC instrument is also observed for the SAA contribution during the NASA-6 mission (TEPC: Q(ICRP60)=1.5) and can be explained by the reduced sensitivity of the TEPC in the very low LET range (Doke et al., 2001b).

Fig. 6 shows details of the count rate during the peak fluxes of the solar particles on Nov 6. Similar structures

were observed by the NASA TEPC instrument (Badhwar, 1998). Due to the lack of MIR position data, our count rates could not be analysed with regard to geomagnetic transmission.

5. Conclusions

The DOSTEL instrument with its silicon planar detectors provided reliable active dosimetry during 87 days for the NASA-6 mission on the MIR orbital station. However, significant differences to results obtained by the NASA TEPC and the NASDA RRMD-III instruments (on similar and equal missions) were found with regard to absorbed dose rates for the GCR and SAA contribution and the mean quality factors derived from the LET spectra. As the dosimetric results depend on several parameters, the comparison of independent measurements of different instruments on different missions may not lead to correct final conclusions. It is very important for a reliable intercomparison that different instruments are exposed during the same mission at the same location behind equal amount of shielding and with well defined viewing directions of the acceptance cones.

Acknowledgements

The authors are grateful to Dr.J.U. Schott (DLR Köln) for his effort as principal investigator of the ADCP experiment. The work in Kiel was financially supported by DLR Bonn under grants 50 WB 9418 and 50 WB 9906.

References

Atwell, W., 2001. Boeing Company, Houston, Private communication.

Badhwar, G.D., 1997. The radiation environment in low-Earth orbit. Radiat. Res. 148, 3–10.

Badhwar, G.D., 1998. NASA JSC, Houston, Private communication.

Badhwar, G.D., Konradi, A., Atwell, W., Golightly, M.J., Cucinotta, F.A., Wilson, J.W., Petrov, V.M., Tchernykh, I.V., Shurshakow, A., Lobakov, A.P., 1996. Measurements of the linear energy transfer spectra on the MIR orbital station and comparison with radiation transport models. Radiat. Meas. 26 (2), 147–158.

Beaujean, R., Kopp, J., Leicher, M., 1995. HZE-Dosimetry in space: measurements and calculations. Radiat. Meas. 25 (1–4), 423–428.

Beaujean, R., Reitz, G., Kopp, J., 1999a. Recent European measurements inside Biroack. Mutat. Res. 430, 183–189.

Beaujean, R., Kopp, J., Reitz, G., 1999b. Active dosimetry on recent space flights. Radiat. Prot. Dosim. 85 (1–4), 223–226.

Doke, T., Hayashi, T., Kikuchi, J., Sakaguchi, T., Terasawa, K., Yoshihira, E., Nagaoka, S., Nakano, T., Takahasi, S., 2001a. Measurements of LET-distribution, does equivalent and quality factors with the RRMD-III on the Space Shuttle missions STS-84, -89, and -91. Radiat. Meas. 33, 373–387.

Doke, T., Hayashi, T., Borak, T.B., 2001b. Comparisons of LET distributions measured in low Earth orbit using tissue-equivalent proportional counter and the position-sensitive silicon-detector telescope (RRMD-II). Radiat. Res. 156, 310–316.

ICRP, 1991. Recommendation of the International Commission on Radiological Protection. Report 60, Pergamon Press, Oxford.

Mueller-Mellin, R., 2001. Kiel University, Private communication.